Available online at www.sciencedirect.com
ScienceDirect
Catalysis Today 129 (2007) 223–230
CATALYSIS TODAY
www.elsevier.com/locate/cattod

Selection of TiO_2-support: UV-transparent alternatives and long-term use limitations for H_2S removal

Raquel Portela [a], Benigno Sánchez [a,*], Juan M. Coronado [a], Roberto Candal [b], Silvia Suárez [a]

[a] *CIEMAT-Environmental Applications of Solar Radiation, Avda. Complutense, 22, Bldg. 42, Madrid, Spain*
[b] *INQUIMAE-UBA-CONICET. Ciudad Universitaria, Pab.2, 1428 Buenos Aires, Argentina*

Available online 27 September 2007

Abstract

Supported-TiO_2 is commonly used for the photocatalytic treatment of gas streams. Nevertheless, selection of the best support is not a trivial task. Cheap, lightweight and easily shaped polymeric materials which are transparent in the TiO_2 activation range (poly(ethylene terephthalate) and cellulose acetate) were used as supports, as an alternative to borosilicate glass or opaque monoliths. The supports were coated with TiO_2 sols containing anatase particles. Different treatments were applied to the sols in order to improve particle crystallinity and wettability on plastic surfaces. The resistance of the coated and uncoated supports against weathering and the photocatalytic activity for elimination of H_2S from polluted air were tested. Both supports were successfully coated with TiO_2. PET supports displayed the higher photocatalytic activity, while TiO_2 caused the degradation of CA supports under UV illumination. The highest activity for H_2S destruction was reached with 20% RH and increasing the temperature of operation in the range of 33–50 °C resulted in higher conversion. Sulfate and SO_2 were detected as byproducts, being the photocatalytic activity reduced when sulfate accumulates on the surface. Different washing procedures for removing the sulfate from the supported photocatalysts were tested. A simple wash with distilled water was found to successfully recover most of the initial activity of the photocatalyst, although basic pH or higher temperatures accelerate sulfate removal.

Keywords: Photocatalysis; H_2S; Supported-TiO_2; Monolithic structures; Polymers

1. Introduction

In photocatalysis, reactor design plays a very important role. Apart from the usual requirements for conventional heterogeneous catalytic reactors (low pressure drop, lack of mass-transport limitations and reduced residence time along with high available catalytic surface) absorption of radiation is required to initiate the reaction and, consequently, the efficiency of the illumination determines the reactor performance. Therefore, a main concern is how to optimize the distribution of the catalyst in the reactor without shading. For photocatalytic treatment of gas streams, the use of powders, very common in water photocatalysis, is generally avoided. Although it favors the contact with the pollutant, the complications of fluidization and separation and the inefficient illumination of the particles are strong drawbacks; therefore, supported-TiO_2 is commonly used. Nevertheless, selection of the best support is not a trivial task, because it should be resistant to oxidizing environments, UV-transparent, generate low pressure drop, facilitate the contact with the pollutant and the photocatalyst must be strongly adhered to the surface. Borosilicate glass or quartz are usual supporting material, because it is transparent in the TiO_2 activation range and facilitates the adherence of the catalyst. Glass reactor walls [1] or glass flat plates [2] are very interesting as supports at lab-scale, but mass transfer limits the flow rates that can be efficiently treated, while Raschig rings [3,4], small tube pieces which provide high geometric surface, facilitate the contact with the pollutant, but produce high pressure drop in the reactor. On the contrary, monolithic structures allow the treatment of large gas volumes, but they are usually made of ceramic or metallic materials and therefore opaque to radiation [5,6]. In this context, cheap, lightweight and easily shaped polymeric materials may be an interesting alternative; the combination of these properties with UV-transparency makes some of them

* Corresponding author. Tel.: +34 913466417; fax: +34 913466037.
E-mail address: benigno.sanchez@ciemat.es (B. Sánchez).

0920-5861/$ – see front matter
doi:10.1016/j.cattod.2007.08.005

very attractive as potential supports, like thin-walled honeycomb structures of poly(ethylene terephthalate) (PET) and cellulose acetate (CA), which are commercially available in a variety of shapes.

The preparation of inorganic thin films on organic supports is currently attracting significant attention [7,8]. Nevertheless, TiO_2-coating of plastic substrates presents several difficulties. The film adhesion is usually poor and thus surface modification could be necessary [9]. Moreover, well-crystallized TiO_2 particles – required to optimize the photocatalytic performance – are usually obtained at treatment temperatures not compatible with thermally sensitive substrates. PET and CA do not withstand temperatures higher than 75 and 145 °C, respectively, without damage. Nevertheless, preparation of liquid suspensions of crystalline TiO_2 particles can be achieved in acidic aqueous solutions [10,11]. This may be employed for deposition of photoactive TiO_2 onto plastics at room temperature using liquid phase deposition techniques, such as dip-coating. On the other hand, photooxidation of polymers reduces their transparency and mechanical resistance [12]. The deposition of SiO_2 between the plastic and the TiO_2 by means of a multi-layer procedure might protect the support from extra photooxidation caused by the radical species generated during irradiation of the photocatalyst. In a previous report by Sánchez et al. [13], two methods of coating PET with a SiO_2 protective layer and then with TiO_2 were presented.

In addition to these difficulties, the possible deactivation of the photocatalysts and the way of regenerating them should be also considered if this technology is expected to have real application. Catalyst deactivation may be reversible when caused by partially oxidized intermediates or weakly adsorbed final products. In these cases, thermally [14] or photocatalytically [15] driven regeneration techniques may be feasible. However, irreversible deactivation may be expected for pollutants containing nitrogen [1], sulfur [16], phosphorus or silicon [17]. The formation of non-volatile final products may demand more aggressive regeneration techniques [1], which may damage the coating. Hydrogen sulfide can be an example. This molecule is a widespread compound released as a by-product of many processes, such as sour gas flaring, petroleum refining, pulp and paper manufacturing or wastewater treatment and is responsible for foul odors and severe damage to health and materials. Consequently, its elimination is a relevant environmental issue, for which there is currently no optimal solution. Previous research has proven that photocatalytic removal of this pollutant is feasible, but SO_4^{2-} has been found to accumulate on the surface of the catalyst [18,19]. The effect of main process parameters on H_2S photocatalytic oxidation (PCO) with TiO_2-coated Raschig rings has been studied in Portela et al. [20]. In this work, we develop efficient procedures of coating UV-transparent polymeric monoliths with photoactive TiO_2 and compare the so-prepared photocatalysts with TiO_2-coated borosilicate glass rings. Their photocatalytic performance in gas-phase H_2S elimination, the aging of the coated polymers and the possibility of regeneration after deactivation are also studied.

2. Experimental methods

2.1. Supports description

Three different supports were studied: (i) borosilicate glass Raschig rings ($L = 13.7$ mm, $d_{ext} = 4$ mm, $d_{int} = 2$ mm) and 9 mm × 9 mm pitch cross-section polymeric monoliths of (ii) PET and (iii) CA. The plastic materials, primarily used as thermal insulators in passive solar systems, were provided by Wacotech GmbH & Co. KG (WaveCore PET150-9/S, wall thickness of 0.15 mm, density of 45 kg/m^3; TIMax CA50-9/S, wall thickness of 0.05 mm, density of 16 kg/m^3). Three monoliths of 2 cm length, with 180 cm^2 of available surface were used in the experiments.

2.2. Synthesis of the sols

A base TiO_2 sol was prepared adding $Ti(iOPr)_4$ (Aldrich) to a vigorously stirred aqueous solution of nitric acid in the proportion 900:6.5:74 (H_2O:HNO_3:$Ti(iOPr)_4$). The system was stirred during 3 days, until a stable and translucent sol was obtained. It was then split in two parts in order to prepare different sols:

(i) Part of the base sol was dialyzed to a final pH of 3.5 using cellulose membranes (3500 MWCO). This sol was named TiO_2-D. Part of this sol was modified by incorporation of 0.01% of Triton. The new sol was named: TiO_2-DTr.
(ii) The rest of the base sol was autoclaved at 150 °C during 12–14 h in a stainless steel calorimetric pump with Teflon walls. After the hydrothermal treatment, the supernatant solution was substituted with water and an exchange step with ethanol was performed, to take advantage of the low surface tension of this solvent [7]. The resultant suspension was ultrasonicated until homogeneity was achieved. It was named TiO_2-HT.

A basic sol of SiO_2 was also synthesized incorporating $Si(OEt)_4$ (98%, Aldrich) with vigorous stirring to an aqueous solution of ammonium hydroxide in the proportions 340:11.2:50 (H_2O:NH_3:$Si(OEt)_4$). The system was stirred until total peptization of the precipitate. The resulting sol was dialyzed to a final pH of 8.0.

2.3. Preparation of the supported photocatalysts

TiO_2 films were prepared by dip-coating the supports several times in the corresponding sol at a withdrawal rate of 0.8 mm s^{-1}. The films were appropriately dried after the application of each layer. In some cases, the supports were coated with a SiO_2 layer before the TiO_2 was applied. The adhesion of SiO_2 to PET was achieved by means of modification of the plastic surface with 1% (v/v) water–ethanol solution of poly(diallyl-dimethyl-ammonium chloride) (PDDA, low molecular weight 20% solution in water supplied by Aldrich). The synthesis conditions and characteristics of the samples are summarized in Table 1.

Table 1
Preparation conditions of the supported photocatalysts

Sample	TiO_2 sol	SiO_2 layers	TiO_2 layers	TiO_2 load (mg/cm^2)	Drying T (°C)	Firing T (°C)
PET-RT	TiO_2-D	0	3	0.16	50	None
PET-trit	TiO_2-DTr	1	3		50	None
PET-HT	TiO_2-HT	1	3		50	None
CA-RT	TiO_2-D	0	3	0.13	50	None
CA-trit	TiO_2-DTr	0	3		50	None
CA-HT	TiO_2-HT	0	3		50	None
Glass rings	TiO_2-D	0	5		90	350

2.4. Characterization of synthesized photocatalysts

The powder X-ray diffraction (XRD) pattern of the TiO_2 xerogel was recorded on a Seifert XRD 3000P diffractometer using nickel-filtered Cu Kα radiation. The UV–vis transmittance was measured by means of a HP8452A diode array spectrophotometer. A scanning electron microscopy (SEM) study of the thin films was carried out in a Zeiss DSM 960 coupled with an EDX Link eXL dispersive energy analyzer; the samples were initially coated with a conductive layer of graphite for analysis. X-ray photoelectron spectra were acquired with a Perkin-Elmer PHI 5400 spectrometer fitted with a monochromated Mg Kα radiation ($h\nu$ = 1253.6 eV) 120 W X-ray source and a hemispherical electron analyzer. The samples were placed on a sample rod, introduced in a pre-treatment chamber, degassed at 25 °C and 10^{-3} Pa for 5 h prior to being transferred to the analysis chamber. Residual pressure during data acquisition was maintained below 3×10^{-7} Pa. The energy regions of the photoelectrons of interest (Ti 2p, S2p, O 1s) were scanned a number of times in order to obtain an acceptable signal-to-noise ratio. Accurate binding energies (±0.2 eV) were determined by referring to the C 1s peak at 284.8 eV. X-ray fluorescence analyses were performed in an Axios (PANalytical) sequential instrument with a single goniometer based measuring channel covering the complete measuring range. Monolithic samples were aged both outdoors (protected by a borosilicate glass from dust and wind) in Madrid between May and September 2006 and in an accelerated weathering chamber QUV (The Q panel Company) following the ASTM G53-88 norm. The weathering chamber submits the samples to continuous cycles of UV-B irradiation (4 h at 60 °C) and water condensation (4 h at 50 °C).

2.5. Photocatalytic activity tests

An annular borosilicate glass photoreactor (d_{int} = 50 mm) placed in vertical position was illuminated by an internal 8-W UV-A lamp (Philips, d_{ext} = 15.2 mm) placed in axial position. The remaining section was filled with either three monoliths or one group of 110 parallel Raschig rings. The continuous inlet gas stream consisted of H_2S (from a calibrated H_2S/N_2 cylinder, Air Liquide) diluted with dry or wet air to obtain the desired concentration of pollutant (35 ppm_v), O_2 (20 ± 1%) and water vapor. Humidity control was achieved by means of a controlled evaporator and mixer (Bronkhorst) and temperature regulation in the photocatalytic system. Liquid- and gas-flow controllers were used to set the flow rates. Analysis of the photoreaction products was performed using a Micro-GC Varian CP-4900 equipped with a micro thermal conductivity detector (μ-TCD) and a CP-PoraPlotQ column (10 m × 0.15 mm). A flow rate of 925 ml/min and a pollutant concentration of 35 ppm_v were selected for the PCO tests performed at around 40 °C and 1 atm of pressure. This means that residence time (t_r) and space time (t_s, calculated as coated surface to molar flow rate ratio) are 0.7 s and 1.2×10^6 s m^2/mol for tests made with 110 rings and 7 s and 2.2×10^6 s m^2/mol for those made with three monoliths. A regeneration technique has been applied to the used photocatalysts. For the plastic supports, it consisted of rinsing of the three monoliths three times with 250 ml of distilled water and almost no agitation. Ionic chromatography analysis of rinsed water was performed to determine the sulfate removed in the washing procedure.

3. Results and discussion

3.1. Catalyst characterization

Fig. 1 shows XRD data for the TiO_2 xerogel obtained from the dialyzed sol dried at room temperature and fired at 350 °C. Although the mean crystalline size estimated by the Scherrer equation is higher after calcination (7.3 nm versus 3.9 nm, which is similar to the one reported by Hu and Yuan [11] for low-temperature synthesis), both patterns show a crystalline phase consisting of anatase with a minor brookite contribution. Thus, acidic peptization and aging of the TiO_2 sol, as previous studies have shown [10,21,13], allows obtaining nanocrystalline anatase at low temperatures, compatible with thermally

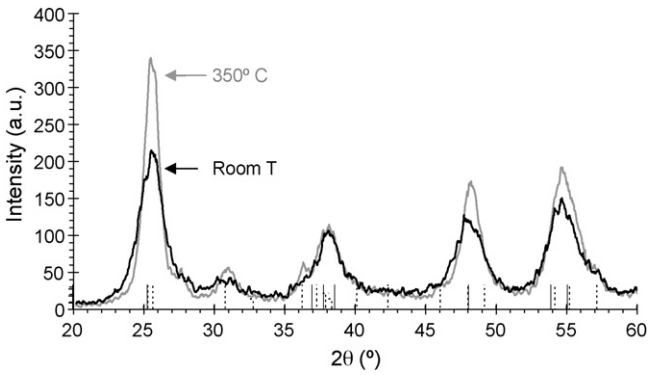

Fig. 1. XRD data for TiO_2 xerogel obtained from the dialyzed sol. Peaks: anatase (–) and brookite (···).

sensitive substrates. Hydrothermal treatment resulted in higher crystallinity, being the mean crystalline size 5.9 nm.

XEDS analysis performed in several points revealed the presence of TiO_2 in the surface of all PET and CA samples. The TiO_2 was homogeneously distributed except for CA-HT and PET–HT, where areas with and without Ti were found. Fig. 2 shows SEM images of CA-RT and PET-RT, where the irregularities observed are those originally present in the plastics and not related to TiO_2 deposits. The samples with triton showed the most uniform appearance.

These results indicate that TiO_2 can be deposited onto both kinds of plastics without surface modification. The amount of TiO_2 on the support after three depositions was 23 mg/monolith (130 μg/cm^2) for CA-RT while it was 30 mg/monolith (160 μg/cm^2) for PET-RT. When the coatings are made using flat structures instead of monoliths, the amount of deposited TiO_2 is much lower around 30–40 μg/cm^2 for all substrates. This is a consequence of the effect of borders in the dip-coating procedure. On the contrary, the deposition of a SiO_2 film was successful only after deposition of a PDDA layer in the case of PET monoliths and ineffective for CA. To obtain crack-free films, 1% (v/v) PDDA solution in 75/25 ethanol/water was used instead of a pure water solution, which leads to cracked films [13], probably due to the low wettability of water on plastics.

The thick lines in Fig. 3 represent the UV–vis transmittance spectra of CA and PET before and after the coating with the dialyzed sol. TiO_2 causes a decrease in transmittance below 350 nm, associated with the band-gap absorption of this semiconductor. Because photodegradation under UV radiation is typical for many polymers [22], the long-term stability of PET and CA catalysts and the influence of the TiO_2 and TiO_2/SiO_2 coatings have been studied outdoors and at the laboratory. Thin and dashed lines of Fig. 3 show the transmittance of the plastic samples after 161 days of exposure to sun and humidity outdoors (Madrid, May–September 2006) and after 160 h of exposure to accelerated weathering under UV-B radiation and water condensation. Uncoated and coated PET presented similar transmission after 161 days of outdoors exposure, loosing 54% and 40% of their initial transmittance at 340 nm(a representative wavelength for PET degradation). PET photodegradation is high due to its strong ultraviolet absorption. The main degradation event is polymer chain scission, leading to evolution of volatile products and generation of carboxyl end-groups [23]. On the other hand, while CA, whose absorption in the UV range is very low, resists quite well the weathering tests, TiO_2-coated CA (CA-RT) has lost 45% of its initial transmittance after being exposed outdoors during 161 days. This means that CA photooxidation is accelerated by TiO_2 and the deposition of a protective SiO_2 layer between the coating and the CA could be useful, because the degradation seems to be caused by the oxidizing species generated in the presence of TiO_2 and not by direct UV radiation, as in the PET case. An alternative way of coating CA with SiO_2 should be investigated. Moreover, the adherence of the TiO_2 layer to CA should be improved, because the aggressive conditions of the weathering chamber resulted in a partial loss of TiO_2, as the transmittance recovery in the TiO_2 absorption range indicates.

Although a direct correlation between accelerated tests and exposure in outdoor environments is difficult to establish, because of the variability and complexity of the outdoor environments, weathering tests are very useful to compare materials under standardized conditions. The accelerated aging of all plastic samples was studied in the weathering chamber for 350 h and HT samples resulted to be the weakest ones, probably because the ethanol treatment caused a partial degradation of the plastics. In general, the samples were very brittle after the treatment and they broke easily. Nevertheless, CA samples still

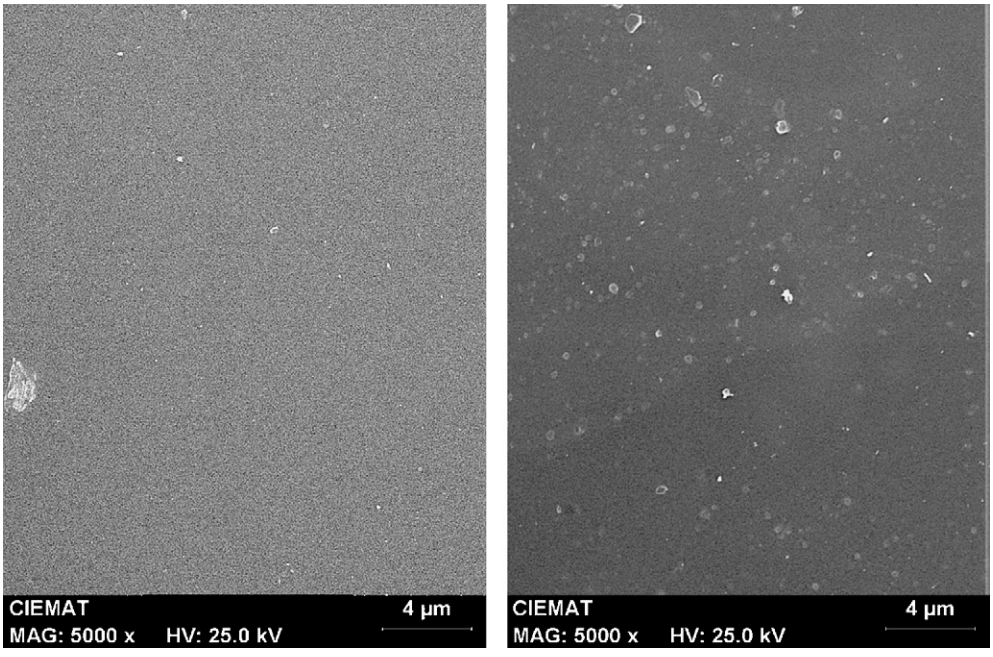

Fig. 2. SEM micrographs of CA-RT (left) and PET-RT (right) coated with 3 TiO_2-layers.

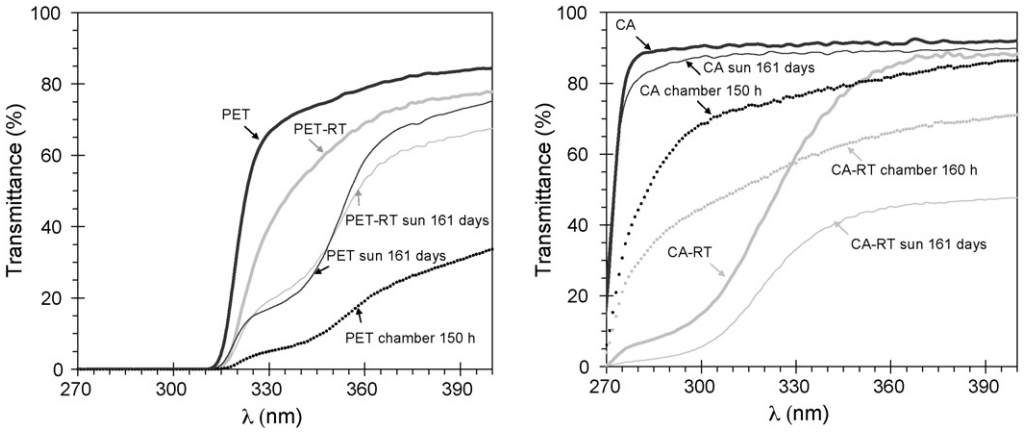

Fig. 3. Aging of PET (left) and CA (right) and effect of the TiO_2 coating. Transmittance of the uncoated (black) or coated (grey) polymers; fresh (thick), after 161 days of sun exposure in Madrid, May–September 2006 (thin) and after 160 h of accelerated weathering (dashed).

showed around the half of their initial transmittance, while PET samples were almost opaque. The severe conditions of the weathering chamber strongly damaged all PET samples, regardless of the coating procedure applied.

3.2. Catalytic activity: effect of relative humidity and temperature

A dark run and an irradiated run without catalyst have proven that both photocatalyst and light are necessary for H_2S destruction. However, an initial decrease in H_2S concentration is observed in the dark due to the adsorption on the photocatalyst for a short period (less than an hour), which duration depends on the humidity of the air stream. PET-RT was the best plastic-supported photocatalyst, although CA-RT presented high photoactivity as well. Their performance at 25% of relative humidity is presented together with the one of 110 fired rings with 5 TiO_2 layers in the same operational conditions (see Fig. 4, left). Although a direct comparison is not possible, due to the differences in coated surface (280 cm^2 for the rings and 540 cm^2 for the monoliths) reactor volume (four times larger for the monoliths.), catalyst mass or flow distribution, it is interesting to observe the differences in the shape of the curves. While all PET-supported catalysts present a maximum in H_2S-conversion after 6–8 h of use and SO_2 begins to be detected after about 2 h, glass-supported catalysts present the maximum after only 3–4 h and SO_2 begins to be detected after 1 h of irradiation. If the used samples are washed and tested again, these time intervals are reduced to less than a half. We suppose that there is an activation of the catalyst, which takes a longer period in the case of non-calcined samples due to the presence of organic residues from the TiO_2 sol. Moreover, if the PET-RT sample is irradiated during 4–5 h in a humid air stream and then tested for H_2S conversion, the maximum almost disappears. In the case of CA, the maximum is not easily observed. It must be taken into account that the adherence of the coating in CA samples is not good and an initial lost of TiO_2 may cause the continuous decay of activity.

The catalysts prepared with the hydrothermal sol submitted to ethanol exchange presented very low activity, despite the higher crystallinity of TiO_2, possibly due to damage to the support caused by ethanol and worse TiO_2 deposition. The presence of the surfactant did not improve the photocatalytic performance of the samples despite the better homogeneity. These photocatalysts exhibited very low initial activity,

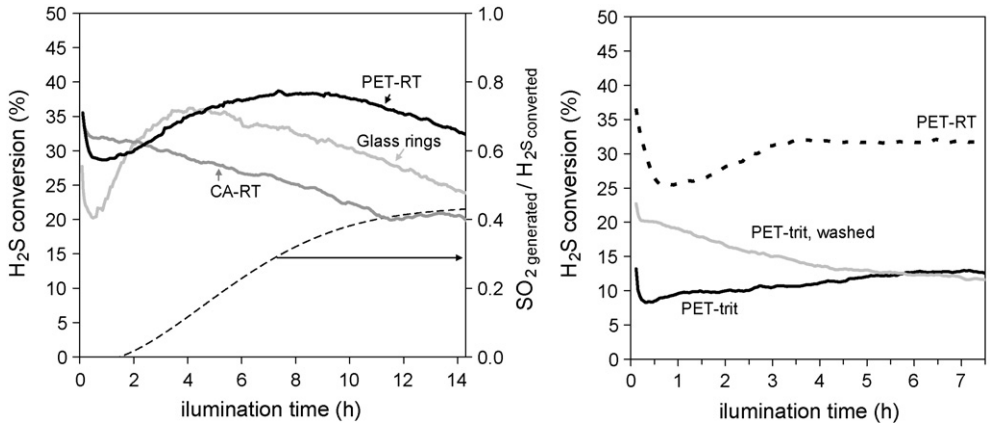

Fig. 4. Photocatalytic activity of supported catalysts. On the left, H_2S conversion obtained at 25% RH with PET-RT (black), CA-RT (dark-grey) and glass Raschig rings (light-grey) and SO_2 generation during PET-RT test (- - -). On the right, H_2S conversion obtained at 50% RH with PET-RT (dashed), PET-trit (black) and PET-trit after the regeneration procedure (grey).

probably due to the competition between H_2S and the surfactant for the oxidant species. Once the surfactant had been oxidized, the photocatalytic activity towards H_2S increased, as can be seen on the right in Fig. 4. The activity of the PET-trit sample in the second use, after regeneration by washing it with distilled water, is higher than in the first use and does not show the initial activation. Samples with the SiO_2 protective layer were in general less active than the ones with only TiO_2.

In order to determine the presence of sulfur compounds on the catalyst surface, XPS experiments were carried out. Fresh and used samples after treatment with a H_2S gas stream were analyzed. The Ti 2p, O 1s and S 2p core levels were measured for rings and CA samples. The analysis of Ti 2p core level showed a peak centered at 458.6 eV assigned to TiO_2 species [24]. No signal of sulfur species was observed on fresh samples, as it was expected. Nevertheless, sulfur compounds were detected in all used samples. The S 2p spectra showed a peak centered at 169.0 eV assigned to sulfate species [24]. These data are related to the O 1s spectra, where the deconvolution of the curve showed two peaks centered at 530.6 and 532.5 eV corresponding to titania and sulfate species, respectively. Although, Canela et al. [19] did not find in H_2S photocatalysis any reaction product except sulfate and Kataoka et al. [18] found only a small amount of SO_2, attributed to sources other than PCO, we have found SO_2 to be an important reaction by-product generated with every photocatalyst tested and at any operational conditions. SO_2 appears in the outlet gas stream after some minutes of reaction and accounts for around half the oxidized H_2S after the conversion reaches the maximum (see Fig. 4). This delay may be the reason why it was not detected in previous studies.

The presence of water vapor plays a key role in the reaction mechanism. H_2O competes with H_2S for adsorption sites [25], but it also increases the activity by means of hole trapping and hydroxyl radical formation. These opposite effects results in the existence of an optimal humidity for which the PCO rate is maximum, which was found to be around 20% (see Fig. 5). This agrees with results for PCO of a similar compound, dimethyl sulfide, for which the highest activity was found to take place at 22% RH [26].

In order to ascertain the mechanism of H_2S PCO and to determine how the involved species are adsorbed, in situ characterization of the TiO_2 surface should be performed. Beck et al. [27] indicate that both H_2O and H_2S are chemisorbed molecularly, while Morterra [28] suggests a mixed type of adsorption, molecularly and dissociatively, and that surface contaminants can change the chemisorption mechanism. Selloni et al. [29] found in a simulation that the adsorption energies for H_2O and H_2S were -0.75 and -0.49 eV. The existence of different types of active sites with different reactivity – as already suggested for the PCO of other pollutants [30,31] – could be proposed, in order to explain the shape of H_2S conversion and SO_2 formation curves. For example, Datta et al. [32] have postulated that on alumina, SO_2 strongly chemisorbs on positively charged metal ions (acidic sites) and negatively charged oxygen ions (basic sites) but when these sites are occupied, a weaker physical adsorption takes place on the hydroxyls. A similar mechanism for TiO_2 could justify the delay in the appearance of SO_2 in the PCO of H_2S. Thus, once the stronger adsorption sites become saturated by the products of H_2S photooxidation (sulfate and/or SO_2), the progress of the reaction would lead to the release of more volatile SO_2 molecules, which then can be only weakly retained by the TiO_2 surface.

Although it has been accepted that PCO is not very sensitive to temperature variations [33], several authors have reported temperature dependant PCO rates at temperatures below 100 °C [34,35]. We have tested the photocatalytic activity at 50% RH and 39.5 °C and then varied the temperature between 35 and 50 °C. At higher temperatures H_2S conversion was significantly better in the range studied. An increase in the reaction rate and the modification of the adsorption equilibrium of the involved species could explain this temperature dependence. The light intensity was monitored during the test and there was almost no variation. Twesme et al. [35] and Zorn et al. [36] also found an improvement in performance from 35 to 77 °C, but not between 77 and 113 °C, which was attributed to the light intensity decrease at those temperatures. As the conversion is a function of illumination time, the relationship between conversion and temperature has been studied in terms of relative variations and was found to be linear ($R^2 = 0.9459$):

$$\frac{x - x_{312.65\,\mathrm{K}}}{x_{312.65\,\mathrm{K}}} = 13.742\left(\frac{T - 312.65}{312.65}\right) + 0.0268$$

where x is the conversion and T is the temperature at the illumination time t and $x_{312.65\,\mathrm{K}}$ is the conversion at

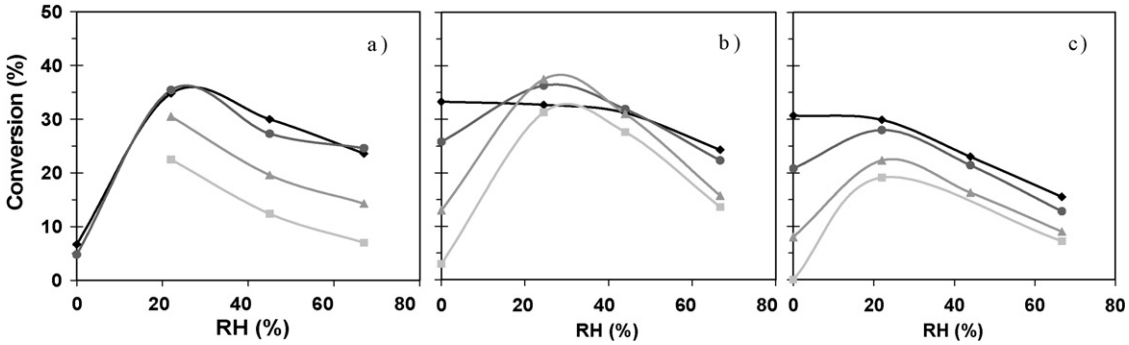

Fig. 5. Effect of relative humidity. H_2S conversion after 3 h (◆), 5 h (●), 10 h (▲) and 15 h (■) of illumination. Catalyst: (a) 110 glass rings; (b) 3 PET-RT monoliths; (c) 3 CA-RT monoliths.

312.65 K at the same time of illumination t. The measured temperature was that of the reactor wall.

3.3. Catalyst deactivation and regeneration

Successful regeneration based on washing the sulfate with water has been achieved for fired TiO_2-coated catalyst. The possibility of optimizing this technique has been investigated. With this purpose, groups of 30 rings used in the same photocatalytic process have been washed in 100 ml flasks varying water volume (10, 25 and 50 ml), pH (2.4, HNO_3 added; 5.6 and 9.2, NaOH added), number of rinses (1–3), agitation rate (0, 50 and 150 rpm), contact time (0–8 min) and temperature (25 and 50 °C). The quantity of sulfate in the rinse water, determined by ionic chromatography, was taken as an indication of regeneration. It has been found that most of the sulfate was removed in the first rinse. Neither longer agitation time nor faster agitation, have significantly improved the sulfate removal, except when compared to no agitation at all. Basic pH and higher temperature slightly favor sulfate removal, but the cost of chemicals and energy does not seem to be worthy. A 25 ml/30 rings was found to be enough volume of water for sulfate removal. The suitability of the washing technique for PET-RT and CA-RT coated monoliths has been investigated as well. The plastic supports coated with three titania layers were used with H_2S and after some hours, when a significant reduction in their photoactivity occurred, were washed and tested again. This process was repeated several times. Fig. 6 displays the conversion after 3 h of illumination of the fresh and several-times regenerated catalysts. Except for the first regeneration of CA-RT, where the lost of activity is very significant, which may be attributed to lost of the photoactive coating, all catalysts seem to recover an important fraction of their initial activity after the recovery procedure. XRF analysis of the PET monoliths showed the presence of S on the plastic surface after use and its strong diminution after the recovery procedure. A small diminution in the Ti content has been observed as well. Vorontosov et al. [37] have reported a similar recovery procedure for gaseous diethyl sulfide PCO with TiO_2 Hombikat UV 100 deposited onto the internal surface of a Pyrex coil. Some permanent catalyst deactivation was noted as well.

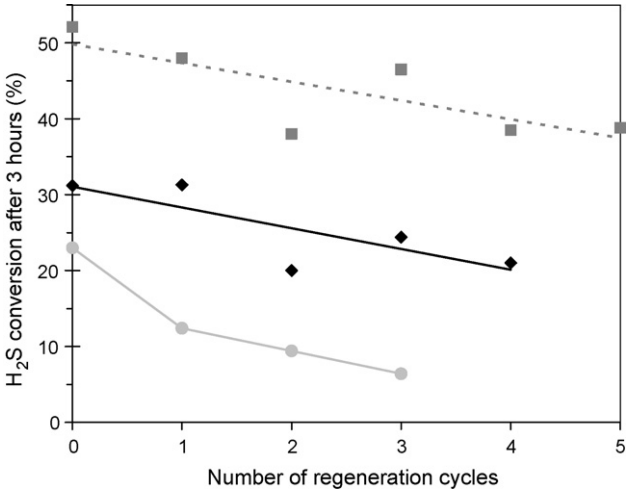

Fig. 6. H_2S conversion for fresh and regenerated photocatalysts as a function of the number of regenerations. Conditions for PET-RT (◆) and CA-RT (●): 925 cm^3/min; 35 ppmv H_2S; 44% RH. Conditions for glass Raschig rings (■): 600 cm^3/min; 35 ppmv H_2S; 20% RH.

4. Conclusions

Photoactive UV-transparent monoliths can be obtained by TiO_2-coating of PET and CA using the sol–gel method. TiO_2 can be directly adhered to the support without a protective layer, although alternatives to improve the mechanical and photochemical resistance of coated plastics, particularly CA, should be investigated. Anatase domains are formed despite the low processing temperature. Using four-times the volume occupied by fired Raschig rings, the TiO_2-coated plastic monoliths present similar photocatalytic conversion for H_2S, being lighter, cheaper and generating lower pressure drop. Smaller channels, more TiO_2 layers or better TiO_2 adherence could improve this performance. An increase in the process temperature in the range between 35–50 °C results in better performance as well, in the treatment of wet air streams. Deactivation occurs in all cases, but PET monoliths seem to withstand a washing recovery procedure similarly to fired catalysts.

Acknowledgments

The authors would like to acknowledge the Comunidad de Madrid (DETOX-H2S S-0505/AMB/0406) CONICET (PIP 5215) and ANPCyT (PICT 10621) for financial support. We aknowledge also María Fuencisla Sánchez for her help in catalysts preparation.

References

[1] C.P. Chang, J.N. Chen, M.C. Lu, H.Y. Yang, Chemosphere 58 (2005) 1071.
[2] G.E. Imoberdorf, H.A. Irazoqui, A.E. Cassano, O.M. Alfano, Ind. Eng. Chem. Res. 44 (2005) 6075.
[3] M.D. Hernández-Alonso, I. Tejedor-Tejedor, J.M. Coronado, J. Soria, M.A. Anderson, Thin Solid Films 502 (2006) 125.
[4] E. Piera, M.I. Tejedor-Tejedor, M.E. Zorn, M.A. Anderson, Appl. Catal. B: Environ. 46 (2003) 671.
[5] M.M. Hossain, G.B. Raupp, A. Tempe, S.O. Hay, T.N. Obee, AIChE J. 45 (6) (1999) 1309.
[6] B. Sánchez, A.I. Cardona, M. Romero, P. Avila, A. Bahamonde, Catal. Today 54 (1999) 369.
[7] M. Langlet, A. Kim, M. Audier, C. Guillard, J.M. Herrmann, J. Mater. Sci. 38 (2003) 3945.
[8] H. Strohm, M. Sgraja, J. Bertling, P. Löbmann, J. Mater. Sci. 38 (2003) 1605.
[9] A. Dutschke, C. Diegelmann, P. Löbmann, Chem. Mater 15 (2003) 3501.
[10] B.L. Bischoff, M.A. Anderson, Chem. Mater. 7 (1995) (1772).
[11] Y. Hu, C. Yuan, J. Mater. Sci. Tech. 22 (2006) 239.
[12] J. Shang, M. Chai, Y. Zhu, Environ. Sci. Tech. 37 (2003) 4494.
[13] B. Sánchez, J.M. Coronado, R. Candal, R. Portela, I. Tejedor, M.A. Anderson, D. Tompkins, T. Lee, Appl. Catal. B 66 (2006) 295.
[14] L. Cao, Z. Gao, S.L. Suib, T.N. Obee, S.O. Hay, J.D. Freihaut, J. Catal. 196 (2000) 253.
[15] J. Peral, D.F. Ollis, J. Catal. 136 (1992) 554.

[16] N. González-García, J.A. Ayllon, X. Domenech, J. Peral, Appl. Catal. B 52 (2004) 69.
[17] J. Peral, D.F. Ollis, J. Mol. Catal. A 115 (1997) 347.
[18] S. Kataoka, E. Lee, M.I. Tejedor-Tejedor, M.A. Anderson, Appl. Catal. B 61 (2005) 159.
[19] M.C. Canela, R.M. Alberici, W.F. Jardim, J. Photochem. Photobiol. A 112 (1998) 73.
[20] R. Portela, B. Sánchez, J.M. Coronado, J. Adv. Oxid. Tech. 10 (2) (2007) 375.
[21] Y. Li, T.J. White, S.H. Lim, J. Solid State Chem. 177 (2004) 1372.
[22] G.M. Wallner, R.W. Lang, Solar Energy 79 (2005) 603.
[23] G.J.M. Fechine, M.S. Rabello, R.M. Souto Maior, L.H. Catalani, Polymer 45 (2004) 2303.
[24] S.W., J.F. Moulder, P.E. Sobol, K.D. Bomben, in: J. Chastain (Ed.), Handbook of X-ray Photoelectron Spectroscopy, second ed., Perkin-Elmer Corp., Physical Electronics Division, Eden Prairie, MN (USA), 1992.
[25] J. Peral, X. Doménech, D.F. Ollis, J. Chem. Technol. Biotechnol. 70 (1997) 117.
[26] K. Demeestere, J. Dewulf, B.D. Witte, H. Van Langenhove, Appl. Catal. B 60 (2005) 93.
[27] D.D. Beck, J.M. White, C.T. Ratcliffe, J. Phys. Chem. 90 (1986) 3123.
[28] C. Morterra, J. Chem. Soc., Faraday Trans. 1 84 (1988), 1617.
[29] A. Selloni, A. Vittadini, M. Gratzel, Surf. Sci. 402 (1–3) (1998) 219.
[30] M. Lewandowski, D.F. Ollis, Appl. Catal. B 45 (2003) 223.
[31] M.J. Backes, A.C. Lukaski, D.S. Muggli, Appl. Catal. B 61 (2005) 21.
[32] A. Datta, R.G. Cavell, R.W. Tower, Z.M. George, J. Phys. Chem. 89 (1985) 443.
[33] M.A. Fox, M.T. Dulay, Chem. Rev. 93 (1993) 341.
[34] D. Bahnemann, D. Bockelmann, R. Goslich, Solar Energy Mater. 24 (1991) 564.
[35] T.M. Twesme, D.T. Tompkins, M.A. Anderson, T.W. Root, Appl. Catal. B 64 (2006) 153.
[36] M.E. Zorn, D.T. Tompkins, W.A. Zeltner, M.A. Anderson, Appl. Catal. B 23 (1999) 1.
[37] A.V. Vorontsov, E.N. Savinov, C. Lion, P.G. Smirniotis, Appl. Catal. B 44 (2003) 25.